

Kinetic Analysis of the Thermal Decomposition of Post-consumer Water Bottles Made of Poly(Ethylene Terephthalate) in a Nitrogen Atmosphere

Nasrollah Hamidi^{1*} and Nurannahaar Abdussalam^{1,2}

¹Department of Biological and Physical Sciences, and 189-Research, South Carolina State University, Orangeburg, USA

²Undergraduate Student, South Carolina State University, Orangeburg, USA

*Corresponding Author: Nasrollah Hamidi, Department of Biological and Physical Sciences, and 189-Research, South Carolina State University, Orangeburg, USA.

Received: June 28, 2021

Published: August 27, 2021

© All rights are reserved by Nasrollah Hamidi and Nurannahaar Abdussalam.

Abstract

91% of all post-consumer plastics are not recycled. Among these plastic wastes are commodities made of poly(ethylene terephthalate) (PET), which comprises the majority of plastics bottles collected as waste. As the plastic wastes continue to increase, they impose a burden on the environment while the products obtained by the pyrolysis under an inert atmosphere save the internal energy and the environment. Harvesting the vast energy content of the single-use post-consumer plastic materials is an art, science, and technology that is under development. This work reports the thermal stability and kinetics of pyrolysis of post-consumer PET (PC-PET) water bottles by thermogravimetric analysis of five samples of PC-PET by variable linear temperature programming. The total weight-loss of each sample was assumed to be in two stages, with each stage corresponding to a one-step conversion of the PC-PET to volatiles. Three methods for determining the kinetic parameters were used: (1) Evaluation and comparison of kinetics parameters (E_a , A and n) from the individual thermograms, (2) evaluation of kinetics parameters using isoconversional methods at the maximum decomposition rate, and (3) evaluation of kinetics parameters overall extent of reaction. In the latter case, 14 $f(\alpha)$ kinetic models were examined at the all α ranges, and the best fit was discussed. Also, Friedman, Kissinger-Akahira-Sunose, and Ozawa-Flynn-Wall methods were applied to the entire range of α and the results were compared. The average energy barrier obtained from all isoconversional models and methods was 189 ± 7 kJ/mol and the difference between highest and lowest obtained E_a was less than 3%, not including $\alpha > 0.90$. The results of this study were compared with other studies including Coca-Cola and Pepsi PET bottles, Costco sprinkling water bottles, commercial-grade PET. Our results were consistent with kinetics data reported in the literature.

Keywords: Postconsumer Plastics; Thermolysis; Kinetics, Model-free Methods: Poly(Ethylene Terephthalate); Water Bottles; Friedman; Kissinger-Akahira-Sunose (KAS); Ozawa-Flynn-Wall (OFW)

Abbreviation	Description
PE	Polyethylene
PET	Poly(ethylene terephthalate)
PC-PET	Post-consumer Poly(ethylene terephthalate)
Tg	Glass transition temperature
TGA	Thermogravimetric analysis
A	Arrhenius pre-exponential factor
α	Extent of a reaction

β	Heating rate (K/min)
E_a	Arrhenius activation energy (kJ/mol)
$E_{a,\alpha}$	Arrhenius activation energy (kJ/mol) related to extent of reaction, α
$f(\alpha)$	differential reaction model listed in Table 1
n	Order of reaction
t	Time
T	Temperature
T_α	Temperature corresponding to a given extent of reaction, α
T_{max}	Temperature corresponding to the maximum rate of decomposition, R_{max} .
r^2	Coefficient of determination of a linear regression. It gives information about the goodness of the fit of a model and is a statistical measure of how well the regression predictions approximate the real data points.

Table a

Introduction

The industrial production of single-use commodities made of synthetic polymer resins, including poly(ethylene terephthalate) (PET) continues to increase [1,2]. As the production of these materials increases, so does the accumulation of post-consumer plastic waste, including PET (PC-PET). Based on EPA data, only about 10% of all plastics are recycled in USA [3]. This accumulated waste is a source of pseudo-renewal material for reuse and recovery of its resin content and its energy content. One way to recover the energy content of plastic waste is to obtain the products of its pyrolysis, which are similar to crude petroleum materials [4]. Thus, it is important to understand the thermal stability of disposed PC-PET as it pertains to recycling and incinerating wastes [5,6]. This is important in the context of thermochemical conversion processes aimed at the use of PC-PCPs as chemical products for recycling or down-cycling under inert atmosphere [7]. and fuel for production of energy [8].

Due to the chemical complexity of polymeric materials, their thermal decomposition involves many different and complex reaction sets. Generally, this complexity has led researchers to study each resin separately. The kinetic analysis must represent the nature of these extremely complex reaction sets in a manageable mathematical way. The kinetics and mechanism of the thermal decomposition of various resins, especially PET, have been studied at varying levels of detail by a great number of investigators

[e.g. 1-40]. Global kinetic analysis has been used successfully to describe the pyrolysis of synthetic polymers and natural polymers. In the case of natural polymers, we can name a few such as cellulose [9], lignin [10]. and hemicellulose [11].

Thermogravimetric analysis (TGA) is an analytical technique used to measure a material's mass loss and thermal stability as a function of temperature and time by monitoring the weight change that occurs as a sample is heated at a constant rate in a controlled atmosphere [12]. The apparent mass loss kinetic models developed so far fall into two categories: [13]. (i) pseudo-single-component overall models (PSOM) [14]. and (ii) pseudo-multi-component overall models (PMOM) [15]. The PSOM regards the PCPs as consisting of a single, pseudo-component, and uses the solid-gas reaction kinetics in the overall temperature range to describe the kinetics of the PCP's weight-loss. In this study the PSOM model was used, taking into account that this model had been used successfully to describe the thermolysis of PET [16-18] and the biomass decomposition processes of almond shells [17,18], pine, eucalyptus woods [18], and other wood species [19]. Nevertheless, PSOM has its limitations due to the global definitions of each of its pseudo components, from which the overall mass loss under experimental conditions cannot be predicted [20].

The major practical purpose of this work was the prediction of process rates and material lifetimes of the PC-PET. The predic-

tions are reliable since sound kinetic analysis methods are used. The theoretical purpose of kinetic analysis of PC-PET is the interpretation of experimentally determined and fundamental theoretical concepts associated with the kinetics of PC-PET, known as the kinetics triplet. In our case, these are the activation energy barrier (E_a), the frequency of vibrations of the activated complex (A), and the reaction mechanism expressed in the form of the functions of the $f(\alpha)$ as defined within the text below and tabulated in table 1s.

The basic aim of the present work was to find an accurate kinetic model suitable for PC-PET weight-loss behavior of very popular lightweight water bottles (~7.7g each) sold by many stores including Sam's Club and Costco. This kind of water bottle is very popular, it is sold under various brands and stores, and we collect them from the recycled beans, and their thermal stability was not available to us. In theory, the kinetic parameters can be obtained from a single experiment [21]. However, both the kinetic parameter and the kinetic model cannot be simultaneously obtained from a single experiment [22,23]. Five temperature scans of five PC-PET samples, instead of one, were used to improve both the discrimination of the reaction mechanism and the determination of the kinetic parameters. We compared the results of this study with many published studies including Coca-Cola and Pepsi bottles, Costco sprinkling water, industrial grade, and pure PET. We did not find a similar study on the thermal properties of this kind of post-consumer water bottle, which this work is about it.

Materials and Methods

The PC-PET used in this investigation came from a 500 mL Member's Mark lightweight water bottle, contain about 7.7 g of PC-PET each. The water bottles were collected immediately after consumption, and prepared for analysis by removal of the label, washing with soap and water, and rinsing with distilled water. The clean bottles were then air-dried and cut to a circular size suitable to fit in a TGA pan. One flat piece of PC-PET was loaded into the TGA sample pan. All samples were near 3 mg (2nd column, Table 1) complying with ICTAC committee recommendation, (sample mass) (heating rate) < 100 mg.K/min [24]. The depth of the sample layer in the pan was equal to the thickness of the PC-PET water bottle, to be less than 0.5 mm and well below the top of the pan. Thermal decomposition was observed in terms of the overall mass loss by using a TGA-7 Thermogravimetric Analyzer (PerkinElmer, Inc., USA). Temperature calibration of the analyzer was carried out by four-point calibration, with special concern since the thermocouple was not in direct contact with the sample in this device. A stream of nitrogen gas was continuously passed into the furnace at a flow rate

of 30 mL/min at room temperature and atmospheric pressure. The temperature program was set to hold at 50°C for 1 min, then incrementally increase to 850°C at the rates (β) of 1, 5, 10, 20, and 40 K/min and held at 850°C for 3 min. The sample mass loss percentages and their temperatures were recorded continuously as a function of temperature and time. The data was downloaded and converted to Microsoft Excel format for further analysis. Experiments were performed twice to ensure reproducibility and the standard error was found to be ± 3 K. Our procedure agreed with the ICTAC Kinetics Committee published the problems and reported the essential principles that should be followed to obtain thermal analysis data that are adequate to the kinetic computations [25].

Each thermogram was divided into two sections; the first section covered the main mass-loss of PC-PET, which was around 85 % PC-PET weight-loss and around 550°C. The second step was the weight-loss above 550°C which was very slow. The fraction of reacted materials (α), also known as the extent of conversion was determined experimentally as:

$\alpha_1 = (\%w_0 - \%w) / (\%w_0 - \%w_{550})$ for the fast step of decomposition and

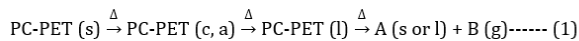
$\alpha_2 = (\%w_{550} - \%w) / (\%w_{550} - \%w_{850})$ for the slow step of reaction,

Where $\%w_0 = 100\%$ is the intimal weight, $\%w$ is the amount of normalized weight at any given temperature, $\%w_{550}$ is the normalized weight at 550°C, and $\%w_{850}$ is the normalized weight at the end of decomposition reaction. The values of α increased from zero to one as the process progressed from initiation to completion. The value of α typically reflects the progress of the overall transformation of a reactant to products, since the physical properties measured by the thermal analysis methods are not species-specific and, thus, cannot be linked directly to specific reactions of the PC-PET molecules.

Theory

A solid bottle made of PET is a mixture of amorphous (a) and crystalline (c) forms of PET, and some fillers and plasticizers. On heating PC-PET (Δ) in differential scanning calorimetry (DSC) or TGA pan under an N_2 atmosphere, the glassy amorphous PC-PET undergoes glass transition (T_g) phase changes as shown in the DSC plot of figure 1s ($T_g \sim 65 - 80^\circ\text{C}$). The resulted amorphous PET upon heating undergoes recrystallization (~140 - 200°C), followed by melting (l) (~230 - 240°C). The initial decomposition and volatilization (g) of PC-PET starts at temperatures above 300°C in a liquid phase (l) rather than a solid phase (s). The kinetics of the

thermal decomposition of PC-PET, which deals with the measurement and parameterization of the process rates, can be expressed by Eq. (1):



The reverse reaction was prevented by increasing temperature linearly and a well-controlled nitrogen stream, which carried the volatiles away as soon as they formed. The thermal decomposition processes that were initiated by a change in heating rate, also known as thermally stimulated processes, usually are parameterized in terms of four major variables: the temperature (T, K), the extent of conversion (α), where (1-α) represents the residual amount of reactant:

$$\frac{d(\alpha)}{dt} = k(T)f(\alpha) \dots\dots\dots(2)$$

The value of α typically reflects the progress of the overall transformation of a reactant to products, since the physical properties measured by the thermal analysis methods are not species-specific and, thus, cannot be linked directly to specific reactions of the PC-PET molecules. The overall transformation, at high temperatures, can involve many simultaneous single reactions and/or, multi-step reactions, each of which has its specific extent of conversion where the slowest reaction determine the overall kinetics of the mechanism, expressed by Eq. (2), even though the mechanism involves more than one step. The temperature (T) changed linearly with time (t), with the constant heating rate (β), controlled by the TGA-7 instruments in agreement with the program settings and the initial temperature (T₀) resulting in the following:

$$T = T_0 + \beta t \dots\dots\dots(3), \text{ where:}$$

$$\beta = dT/dt \dots\dots\dots (4)$$

The heating rate dependence of the instantaneous conversion of the PC-PET can be expressed by using a wide variety of reaction models, f(α) [26], published widely by many authors; the most common of which are presented in table 1s. The reaction models are of three major types: accelerating (A), decelerating (D) and sigmoidal (σ) or autocatalytic, as shown in figure 1a, according to the published literature [27-32]. Accelerating models represent processes whose rates increase continuously with increasing extent of conversion and reaches its maximum at the end of the process (Figure 1a (A)). Models of the decelerating type represent processes whose rate has its maximum at the beginning of the process and decreases continuously as the extent of conversion increases

(Figure 1a (D)). The sigmoidal models represent processes whose initial and final stages demonstrate, respectively, the accelerating and decelerating behavior. The sigmoidal process rate reaches its maximum at some intermediate value of the extent of conversion, α, as its reaction profile in figure 1a (σ) shows. The PC-PET model profiles displayed in figure 1b showed a series of identical curves, displaced from one another on the time axis, similar to the sigmoidal curve in figure 1a. The similarity of the α profile of PC-PET in figure 1b to the sigmoidal α profile in figure 1a indicates that the pyrolysis of PC-PET followed a sigmoidal reaction profile.

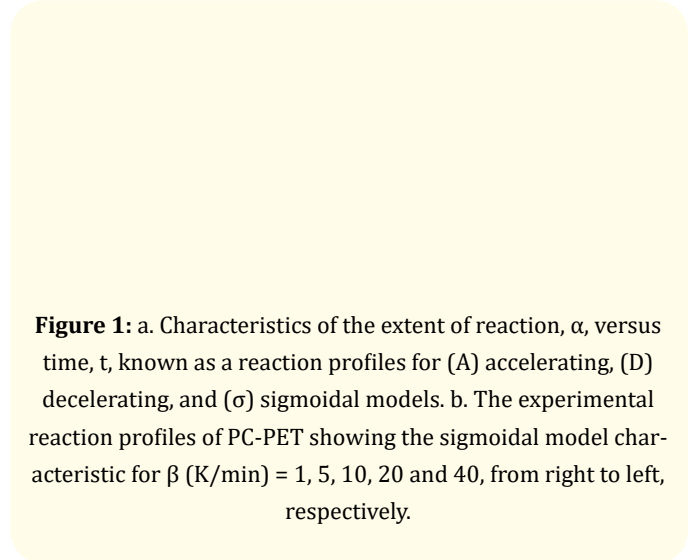


Figure 1: a. Characteristics of the extent of reaction, α, versus time, t, known as a reaction profiles for (A) accelerating, (D) decelerating, and (σ) sigmoidal models. b. The experimental reaction profiles of PC-PET showing the sigmoidal model characteristic for β (K/min) = 1, 5, 10, 20 and 40, from right to left, respectively.

The f(α) value in equation (3) for the sigmoidal reactions follows a power type model, such as equation (5) [38]:

$$f(\alpha) = \alpha^m (1-\alpha)^n [-\ln(1-\alpha)]^p \dots\dots\dots(5)$$

Where n being the reaction order, with m = p = 0 and n = 1, is for first-order reactions and called Mampel model (Table 1s, 2nd column). In the case that the k(T) in equation (2) follows the Arrhenius expression, its value is given by Eq. (6), for rate constant:

$$k(T) = A \text{Exp}(-E_a/RT) \dots\dots\dots(6)$$

Where A is the pre-exponential factor of Arrhenius, E_a is the activation energy of the reaction, R is the universal gas constant R = 8.314 J/(mol K) and T is the absolute temperature (K). Combining equation (2) and (6) yields:

$$(d\alpha/dt \equiv \dot{R}) = k(T)f(\alpha) = f(\alpha) A \text{Exp}(-E_a/RT) \dots\dots\dots(7)$$

Equation (7) is the basis for the various differential kinetic methods. It applies to any temperature program, be it isothermal

or non-isothermal. According to equation (8), the slope of a plot of $\ln[(d\alpha/dt)/f(\alpha)] = \ln k$ versus $1/T$, known as an Arrhenius plot, yields the value of $(-E_a/R)$, and the intercept is the value of $\ln A$.

$$\ln[(d\alpha/dt)/f(\alpha)] \equiv \ln k = -E_a/RT + \ln A \text{-----(8)}$$

Taking $f(\alpha) = (1-\alpha)^n$, equation (11) becomes (applies to first order reactions, $n = 1$, model F1, Table 1s):

$$\ln[\check{R}/(1-\alpha)^n] = -\frac{E_a}{RT} + \ln A \text{-----(9)}$$

Under linear heating rate (β) conditions, the general equation for the various differential kinetic models can be obtained by combining equation (4) and (7) which can be written as:

$$\frac{d\alpha}{dT} = \frac{A}{\beta} \text{Exp}\left(-\frac{E_a}{RT}\right) f(\alpha) \text{-----(10)}$$

Differentiation of the above equation (Eq.10) with respect to T yields:

$$d^2\alpha/dT^2 = (A/\beta)[(E_a/RT^2)f(\alpha)+f'(\alpha)]\text{Exp}(-E_a/RT) \text{-----(11)}$$

Where $f'(\alpha) = 1$ is the derivative of $f(\alpha)$ for the first-order reactions. At the maximum reaction rate the value of equation (11) approaches zero according to the derivatives rules. Redhead [28] solved equation (11) to find the temperature (T_{max}) at which the reaction rate is maximum for the kinetics of thermal desorption of gases. The solution for a first-order reaction, assuming that E_a is not a function of α , results in:

$$\beta T_{max}^{-2} = (AR/E_a)\text{Exp}(-E_a/RT) \text{-----(12)}$$

Kissinger [29] used the logarithmic form of equation (12) at R_{max} to analyzing TGA data as:

$$\ln(\beta T_{max}^{-2}) = \ln[(-AR/E_a)f'(\alpha_{max})] - E_a/RT_{max} \text{----- (13)}$$

Where $f'(\alpha) = df(\alpha)/d\alpha$. Eqn. (13) originates from the basic rate equation of a single-step process, equation (7).

To obtain the value of E_a at a given value of α , $E_{a,\alpha}$, as a function of conversion, the Kissinger-Akahira-Sunose (KAS) method often is used by representing $\ln(\beta T_{\alpha}^{-2})$ vs $1/T_{\alpha}$ in which T_{α} is the temperature for specific values of the α :

$$\ln(\beta T_{\alpha}^{-2}) = \ln(AR/E_{a,\alpha}) - E_{a,\alpha}/RT_{\alpha} \text{----- (14)}$$

The other frequently used isoconversional method known as the Friedman method (F), is based on Eq. (7), also estimates the value of E_a at a given value of α ($E_{a,\alpha}$), from the

slope of a logarithmic plot of the rate of reaction at a given value of α (R_{α}), and its corresponding temperature (T_{α}), according to equation (15):

$$\ln R_{\alpha} = \ln A + \ln f(\alpha) - E_{a,\alpha}/RT_{\alpha} \text{----- (15)}$$

The Flynn-Wall-Ozawa method is another model-free method that was obtained by rearranging and integrating the Arrhenius rate law equation (7) and then applying Doyle approximation [30] to obtain equation (16). The plot of $\ln \beta$ versus $1/T$ gives a straight line with the slope $-1.052E_a/R$ [38]:

$$\ln \beta = \ln[0.0048AE_a/Rg(\alpha)] - 1.0516E_a/RT \text{-----(16)}$$

Where $g(\alpha)$ is the integral form of kinetic model (i.e. $g(\alpha) = kt$).

Results and Discussion

Characteristics of the weight-loss curves

Figure 2a shows the normalized TGA thermograms of PC-PET samples at the indicated β values. The negative derivatives of TGA curves with time, which correspond to the rate of weight-loss, \check{R} , are represented in figure 2b. As the curves in figure 2a and 2b show, all the samples subjected to pyrolysis under nitrogen were identical in shape except for the displacement of one curve from the other along the temperature axis. This observation suggests that the same order of reaction may have prevailed over the whole heating rate range.

Thermal stability

The characteristic quantities that have been considered to be relatively reliable criteria for thermal stability are the initial decomposition temperature (T_i) at which 98% of the weight of polymer remained, 90%, the half-weight loss temperature, 50% and the final decomposition temperature (T_f) [31,32]. These characteristics temperatures have been widely adopted in the literature. In the case of PC-PET, the values of T_f were estimated as the value when the TGA curve showed a plateau, which was around 85% weight-loss. To study the kinetics of decomposition, the maximum decomposition rate, R_{max} , its corresponding temperature, also known as the peak temperature, T_{max} , and the extent of reaction at the R_{max} known as α_{max} [33], are considered to be reliable characteristics as listed in table 1.

The results in table 1 underscore that the polymer stability degradation temperatures increase regularly with increasing heating rate. These data reveal that there is a positive correlation between the initial decomposition temperatures ($T_{98\%}$ or $T_{90\%}$) and the heat-

ing rate of the samples. For example, the initial decomposition temperature, $T_{98\%}$, varied; it was 348°C for the heating rate of 1 K/min and 419 °C for the heating rate of 40 K/min (3rd column of table 1). The values of initial decomposition temperatures ($T_{90\%}$ = 372, 403 and 418°C, 4th column of table 1), and the ending decomposition temperatures, (T_f = 444, 478 and 510°C, 7th column of table 1) obtained in this study for heating rates of 1, 5 and 10 K/min, respectively, agree with the reported temperatures for pure PET films in other studies, with $T_{90\%}$ being about 380, 420 and 435°C and the ending decomposition temperatures, T_p , being about 450, 475 and 505°C at heating rates of 1.25, 5 and 10 K/min, respectively [34]. The residual weight of the dark char-like remains of PC-PET (last column of table 1) was found to be ~13-14% of the original sample at 550 °C, but it was not dependent on the heating rate. However, our ~13-14% residual weights at 550 °C (11th column of table 1) were slightly higher than the reported values (about 10%) for pure PET films in the above references. [16]. This may be due to the additives that the manufacturer applied to the original resins to make the bottle.

The evaporation of volatile chemicals that occurred in the temperature range of 50 - 300°C are not appreciable in the actual y-axis scale, and constituted less than 0.5% weight-loss for all the PC-PET.

The rate of weight-loss

Figure 2b shows that the thermal degradation process of PC-PET under an inert nitrogen environment had one distinct rate curve for each of the five rates used. This behavior was similar to pure PET [16], PC-PET [18,35], and other synthetic polymers such

Figure 2: TGA and \dot{R} thermograms for the decomposition of PC-PET in a nitrogen atmosphere at the β = 1, 5, 10, 20, and 40 K/min, from left to right, respectively. (a) Normalized weight loss; (a2) enlargement of thermograms corresponding to temperature range 500-850°C. (b) variation of \dot{R} with temperature, (b1) expansion of 350-550°C to show \dot{R} at β = 1, and 5; and (b2) enlargement of the \dot{R} at temperatures above 500°C.

Sample	M_{sample}	β	$T_{98\%}$	$T_{90\%}$	$T_{50\%}$	$T_{20\%}$	T_f	R_{max}	T_{max}	α_{max}	$W_{\%550}$ °C
1	3.496	1.0	348	372	401	423	444	2.86	401	0.62	13.85
2	3.796	5.0	377	403	433	455	478	11.80	434	0.62	14.14
4	3.369	10.0	393	418	449	470	510	23.47	450	0.62	14.18
7	3.155	20.0	408	433	463	483	529	44.38	463	0.58	13.24
13	3.122	40.0	419	443	476	496	555	84.14	480	0.68	12.81

Table 1: Features of the thermogravimetric curves for PC-PET samples in nitrogen including the original sample weights, M_{sample} (mg), β (K/min), $T_{98\%}$, $T_{90\%}$, $T_{50\%}$, $T_{20\%}$ and T_f (all in °C), the R_{max} (%/min) and its corresponding T_{max} (°C) and α_{max} , and the residual mass of PC-PET at 550°C.

as polyethylene, polypropylene [36], and polystyrene [37]. These all show one main, distinct weight loss step, which suggests that all of them may have a similar degradation mechanism [38]. Moreover, the weight-loss of PC-PET did not completely stop after the fast decomposition step which covered the initial 85% of weight-loss; it

continued very slowly, showing the second step of slow mass loss at temperatures above 450°C as depicted in the expanded sections of the figure 2a (a2). In the same manner, figure 2b shows the decomposition rate curves for this stage versus temperature at its expanded section (b2) demonstrated one common shape.

Temperature at the maximum weight-loss rate

One of the parameters that characterize the displacement of the individual curves within the family of curves of figure 2b is the T_{max} , the temperature at which the rate of reaction reached its highest value. The values of T_{max} for the 5 heating rates employed in this study are shown in table 1, column 9. As the value of β increased, the value of T_{max} also increased towards higher temperatures, ranging from 401°C when the heating rate was 1 K/min, to $T_{max} = 480$ °C when the heating rate was increased to 40 K/min. following a logarithmic path as shown in figure 4(d). A possible reason for the displacement in T_{max} is that the true sample temperature lags behind that recorded by the instrument at higher heating rates. The origin of this is due to the heat capacity of the sample and the heat transfer effects, as well as the association time of the reactant materials in the TGA pan before vaporization. This rationale can also be applied to explain the displacement in R_{max} .

The maximum weight-loss rate

The R_{max} data in table 1, 8th column show that the rates of the degradation were not identical at each and every β . From a maximum rate of 2.86 %/min. at the $\beta = 1$ K/min., the reaction rate increased to the maximum rate of 84.14 %/min. at the $\beta = 40$ K/min. The dependence of R_{max} on heating rate was perfectly linear, a rapidly increasing function, $R_{max} = f(\beta)$, described by Eq. (1A) with a slope near to the β scales, 5, 10, 20, and 40 in this experiment but excluding the $\beta = 1$.

$$R_{max} = 2.0774\beta + 1.7531 \text{ with } r^2 = 0.9991 \quad \text{-----(1A)}$$

The values of α_{max} (Table 1, 10th column) show that the maximum rate of reaction at any heating rate was attained only after the extent of reaction passed the value of $\alpha = 0.6$; i.e. after more than half of the original PC-PET had decomposed; and the values of α_{max} changed with heating rates randomly, between 0.6 and 0.7 indicating an asymmetric character of \dot{R} versus α .

Evaluation of kinetics parameters from a single thermogram

The arrhenius plots

Figure 3 shows the Arrhenius plot of thermal degradation of PC-PET at $\beta = 40$ K/min under a nitrogen atmosphere according to equation (7). The thermal degradation of PC-PET, below and above 500°C displayed as two distinguishable regions. Above this temperature (500°C) the weight-loss process of PC-PET is extremely slow, illustrated in the left region of the plot. It is so slow that most of the researchers did not report data from this region as a weight-loss region. An interesting feature of the Arrhenius plots in figure

3 is that there are three to four segments for each region. The segmented curve describing the decomposition reaction of PC-PET at the temperatures below 506°C showed a section at lower temperatures with a slope near to zero, where there was no-weight-loss (50 - 362°C), followed by a sector with a finite slope (362 - 501°C, 2nd and 3rd columns table 2) where the main weight-loss occurred, and ending in a section with very high slope (501 - 506°C) where the decomposition rate plateaued. The segmented decomposition curve at the second region (511- 850°C) showed four segments: a small segment with a positive slope (511 - 572°C), before the section of the zero slope curve (572 - 705°C). This is because the decomposition reaction did not stop at 511°C, and it was only in a fast deceleration process. This was followed with a segment of the finite slope, 703 - 843°C, and ended with a segment of a very high slope, 843 - 850°C. Similar thermal degradation behavior was observed for the other four heating rates in this study. To avoid over-crowding in figure 3, the total Arrhenius plot of 40 K/min was shown.

Figure 3: The segmented Arrhenius plot of PC-PET thermal decomposition (50 to 850 °C) at the $\beta = 40$ K/min.

Evaluation of the reaction order (n)

The determination of the values of n was by trial fit using a least-squares fit program, by judging the highest value of the coefficient of determination of the linear regression, r^2 , of the corresponding data. The values of r^2 are very sensitive to the corresponding values of n . It is possible to find the best value of n to fitting into TGA data by plotting the values of r^2 obtained from equation (9) versus corresponding n values, as shown in the plot of figure 5s. Using this method, it is easy to discriminate between the various values of n to within 5%. The results of this study showed that applying the

value of $n = 1.00$ into equation (9) was unsatisfactory for all β s, as presented in the 4th column of table 2.

Evaluation of n , E_a and $\ln A$ from individual thermograms

Though the recommendation of the ICTAC Kinetics Committee, the evaluation of kinetics parameters base on a single heating rate is not precise, however, we did it for comparison [31,32]. The values of apparent kinetics triplet (E_a , A and n) were calculated from the finite slope regions of the Arrhenius plots, tabulated in table 2. Also, other features of the Arrhenius plots including β (K/min.), T_i and T_f (°C), initial and final temperature of the segment, respectively, α_i and α_f , initial and final values of the extent of the reaction for the segment, respectively are tabulated in the same table.

The values of n (4th column of table 2) which were obtained from the maximum of r^2 vs, n curves shown in figure 3s showed that, indeed, the thermal degradation process did not follow first-order kinetics, i.e., $n = 1.00$. The ranges of the extent of reaction (α_i and α_f) that belonged to these range of temperatures were noted in the 7th and 8th columns of table 2, respectively. At the lowest heating rates, the breakpoint (T_b , 2nd column) moved to lower temperature compared to the T_i at the higher β values.

An immediate benefit of the segmented Arrhenius plot (Figure 3) is the ability to obtain and compare kinetic parameters, i.e., n , E_a and A , at the various heating rates as tabulated in table 2. Both n and E_a (5th and 6th columns of table 2) were decreasing by increas-

β	T_i (°C)	T_f (°C)	n	E_a (kJ/mol)	$\ln A$ (min ⁻¹)	α_i	α_f
1	354	427	1.952	348	64.745	0.037	0.979
5	340	490	1.680	318	58.126	0.011	0.999
10	362	468	1.500	304	55.099	0.012	0.919
20	375	477	1.470	299	53.788	0.009	0.841
40	392	501	1.235	283	50.981	0.022	0.944

Table 2: Features of the Arrhenius plots of pyrolysis of PC-PET in nitrogen including β (K/min.), T_i and T_f (°C), n , E_a , A , α_i and α_f .

ing the value of β ; the same behavior was reported for the thermal degradation of pure PET [16]. Also, the value of E_a increased as the values of $\ln A$ and n increased. These pairs of (E_a , $\ln A$) and (E_a , n) data fit in a straight line as shown in figure 3s, which is within expectations. Apparently, the increase in the values of E_a was compensated by a corresponding increase in the value of n , and $\ln A$ as has been shown in figure 3s and by other researchers [16,39,40]. For a given simple reaction the value of E_a is independent of the value of β , so the change in the values of E_a is due to the values of n and A .

Saha and Ghoshal [41], who studied the thermal degradation of Coca Cola and Pepsi PET-bottles, evaluated the value of E_a at around 70 - 80% weight loss in the temperature range of 653-788 K (380 - 515°C the same range of temperatures of this work) to be 322 and 339 kJ/mole, for the two types of bottles, respectively, for the n^{th} order pyrolysis model. These values are near to the E_a values that were obtained for the PC-PET water bottle in this work when the values of n were 1.60, and 1.95 (2nd and 3rd row of table 2).

The observed variation of the kinetic parameters of PC-PET with β , is due to the coupling of physical processes and chemical processes, as shown in a larger context in the kinetics of heteroge-

neous reactions [42]. In the case of PC-PET pyrolysis, the chemical processes are primarily bond-breaking and bond-forming, with the consequent production of many gaseous, liquid and solid products. In turn, this gives rise to high concentration differences between the reaction front and the inert fluid atmosphere. Thus, the physical process involved in the degradation process, which includes the heat and mass transfer effects, would be significant and should depend on the extent of the decomposition reaction. Additionally, the porous dark surface layer of the degraded material grows both in thickness and area with the progression of the reaction front, which affects the transfer of heat into the material.

Methods based on the maximum rate of decomposition

The R_{max} methods provide a very simple way of estimating the activation energy and as a routine followed by the majority, but this is not guaranteed to yield the best or even simply a correct result since the methods undermining that thermally stimulated processes are commonly multi-step reactions [43]. Also, these methods are not among the techniques recommended for advanced kinetic studies [28] most of the time, they are employed in materials characterization work that among other quantities reports a number that presumably characterizes an energy barrier to a thermal pro-

cess under study. In the following, the kinetics parameters will be evaluated using three frequented used methods and they will be compared with each other. The data used in this work comply with the accepted Redhead statement that β should be varied by at least 2 orders of magnitude for reasonable accuracy of the results.

Kissinger method

The Kissinger (K) method [29] has been recognized as the most popular way of evaluating the activation energy of thermally stimulated processes. The method was introduced as a routine and followed by the majority [43]. The slope of a plot of $\ln\beta T_{\max}^{-2}$ versus $1/T_{\max}$, Eq. (14), yields $-E_a/R$ assuming the thermal degradation process being the first-order one as shown in figure 4(a). The values of $\ln A$ from the intercept ($\ln(AR/E_a)$), and E_a obtained from the slope of the plot of figure 4(a) are tabulated in the 2nd row, 2nd, and 3rd columns of table 3, respectively. The value of $E_a = 186$ obtained from the KG method is in the range of average $E_a = 188 \pm 5$; when the model-free method (see section 5.4.1) was applied to the thermal degradation data (Table 2s). It was also found that the corresponding value of $\ln A = 30.13$ obtained from the K method (Table 3, 2nd row) was smaller than the obtained values from other methods (Table 3s).

Method	E_a (kJ/mol)	ln (intercept)
K	185.9	30.13
OFW	197.7	25.17
F	181.8	33.93

Table 3: Comparison of the values of the E_a and $\ln A$ obtained from the Kissinger (K), Ozawa-Flynn-Wall (OFW), and R_{\max} versus $1/T_{\max}$ (F) methods.

es over α ranges and at the R_{\max} . The slope of the straight line of a plot of $\ln(\beta)$ versus $1/T_{\max}$ gives $1.0518E_a/R$ as shown in figure 4(b) [22,23]. The values of the intercept and the E_a obtained from this method are tabulated in the third row of table 3. The apparent $E_a = 189$ kJ/mol value obtained from this method was slightly higher than the values of $E_a = 186$ kJ/mol obtained from the KG method, in section 4.3.1. The value of the intercept being equal to $\ln[AE_a/Rg(\alpha_{\max})] = 35.25$ was closed to the value of $\ln A = 34.41 \pm 0.49$ from model-free method. Assuming $g(\alpha_{\max}) = 1$, the calculated value of $\ln A = 24.25$ is the smallest among all methods. The large difference in the values of $\ln A$ is justified due to the assumptions that each method imbibed in the intercept.

Friedman (F) method at R_{\max} and T_{\max}

The Friedman method (Equation 15) evaluates reaction energy barrier over the α range, however, could be applied to R_{\max} to get a single E_a value. The slope of the plot of $\ln R_{\max}$ versus $1/T_{\max}$ (Figure 4(c)) results in the value of $-E_a/R$. The value of $E_a = 182$ kJ/mol from this method is slightly smaller than the values of E_a obtained from the previous two methods. These values are tabulated in the 4th row of table 3 for comparison. The intercept values 33.44 is a combination of $\ln A$ and $\ln f(\alpha_{\max}) \sim (1-0.61)$; the calculated $\ln A = 33.93$ is larger than the one obtained by the KG method.

Evaluation of kinetic parameters for entire extent of the reaction

The major advantage of these methods is that they do not require any assumptions concerning the form of the kinetic equation other than the Arrhenius type temperature dependence to calculate the E_a value.

Model-free kinetics methods

The form of equation 7 indicates that the obtained values of E_a are independent of $f(\alpha)$ functions; this method is often called the model-free method. From the slope and intercept of a plot of $\ln[\ddot{R}/f(\alpha)] = \ln k$ versus $1/T$ ($1/K$) at a given α value with the appropri-

Figure 4: (a) Kissinger Method, (b) Ozawa-Flynn-Wall method, (c) $\ln R_{\max}$ versus $1/T$ (Friedman method), and (d) $\ln \beta$ versus $\ln T_{\max}$ of PC-PET.

The Ozawa-flynn-wall (OFW) at T_{\max}

The Ozawa-Flynn-Wall (OFW) isoconversional method has been used frequently to evaluate E_a of pyrolysis process-

ated $f(\alpha)$, the value of E_a and $\ln A$ are obtained, simultaneously. The order of the reaction is known by the form of the $f(\alpha)$ function. Figure 5 is such a plot for the extent of reaction at $\alpha = 0.50$ where $f(\alpha)$ functions tabulated in table 1s were embedded into equation 7. The adjusted lines to the experimental data in figure 5 are all parallel to each other, demonstrating that the values of E_a were independent of the models used, as was expected. However, the frequency factor which is obtained from the intercept of each line which represented the value of $\ln A$ were depending on the model used, as shown in table 3s, which is within the expectations. The variation of the $\ln k$ with the inverse of temperature, for the temperatures above 550°C are not shown. Table 2s shows the values of E_a obtained for the 14 models of reactions, $f(\alpha)$, covering a wide range of α s, $0.05 < \alpha < 0.95$, and corresponding to heating rates ranging from 1 to 40 K/min with their corresponding r^2 values shown in figure 5s. These E_a values were near to each other, independent of the $f(\alpha)$ function used for a given α value as shown in the distribution of these data points in figure 6. For example, the average E_a obtained from the slope of all models for $\alpha = 0.50$ was $E_a = 193.3 \pm 0.1$ kJ/mol (8th row table 2s). This indicates that E_a is independent of the form of $f(\alpha)$, the model used, which was within expectations. The dependency of E_a versus α starts with the lowest value $E_a = 183$ kJ/mol at the initial step of decomposition, $\alpha = 0.05$, the value of E_a increased by increasing the extent of reaction reaching a plateau around $\alpha \sim 0.2$, $E_a = 190$ kJ/mol; then started to decrease at $\alpha > 0.85$ to a minimum value of 175 kJ/mol at $\alpha = 0.95$. The corresponding values of $\ln A$, the intercepts of the graphs, are tabulated in table 3s, also showed a similar trend as that seen in E_a , as shown in figure 7. These values were scattered compared to E_a values, and they depended on the model used.

In the case of PC-PET, for all values of α and all models presented in table 1s, the variation of $\ln k$ versus $1/T$ yielded a straight line for a given value of α as was shown by the graphs in figure 5. Though, the r^2 values of the models were not similar. Figure 5s compares the variation of the values of r^2 for all models at a given α value; according to the numbers corresponding to the kinetics models presented in table 1s. According to figure 5s the highest r^2 values were observed for the kinetic model 5 (D1), and 13 (D2) for $\alpha = 0.05$ to 0.40 corresponding $f(\alpha)$, being $[1/(2\alpha)]$, and $1/[-\ln(1-\alpha)]$. Model 10 (D3) with $f(\alpha) = (3/2)(1-\alpha)^{2/3}[1 - (1-\alpha)^{1/3}]^{-1}$ was the best for $0.05 < \alpha < 0.60$. Whereas models 1, 2, and 3 corresponding to the power-law P4 ($4\alpha^{3/4}$), P3 ($2\alpha^{2/3}$), and P2 [$2/(3\alpha^{1/2})$]. were best feet for $\alpha > 0.65$. F1 model, was fitted better to $\alpha = 0.95$. The best fitting of the different reaction models to the different extents of reactions could be an indication of the dependence of the degradation mechanism

Figure 5: Application of Eq. (7) using the $f(\alpha)$ functions of Table 1s to the PC-PET thermal decompositions data for $\alpha = 0.50$. Similar plots were obtained for the other α values which were omitted to save space.

on the α value. This could be justified by considering that at each extent of the reaction, the composition of reactants was changed since the original PC-PET was converted to non-volatile sub-chains and longer chains, in the thermal degradation process. In this manner, the materials under the study at the various extent of reaction differ from each other. The published literature supports that the compositions of the pyrolysis products varied according to the pyrolysis temperature [e.g. 44].

Figure 6: Variation of the values of E_a as a function of α for the PC-PET obtained from the slope of plots of $\ln k$ versus $1/T$ using models listed in Table 1s, Friedman (FM), FWO, and KAS methods.

The inherent, general assumption imbibed in equation (7) is that all processes have an Arrhenius temperature dependence. The experimental kinetic parameters obtained by these kinds of assumptions are called “effective”, “apparent”, “empirical”, or “global” since they are different from intrinsic parameters. For example, the effective activation energies estimated for PC-PET, listed in table 2s, and shown in figure 6 are most likely to be a composite value determined by the sum of activation energy barriers of the involved individual steps. The effective activation energy can vary strongly with the temperature and the extent of conversion [45,46] or take on negative values [47] such as the case of PC-PET at the initial steps of slow degradation at a temperature around 500°C as shown in figure 3. Such discrepancies are not typically expected for the E_a of a simple elementary individual type of chemical reaction.

Friedman method

Figure 7 shows the graphic representations of $\ln R_\alpha$ versus $1/T_\alpha$, the isoconversional method known as the Friedman method, expresses by equation (15). The slope of these plots results in the value of the energy barrier at a given extent of reaction, $-E_{a,\alpha}/R$. The intercept is a combination of $\ln A$ and $\ln f(\alpha)$. As figure 6 shows, the variations of the values of $E_{a,\alpha}$ for PC-PET obtained from the Friedman method were similar to the E_a obtained from other; they following similar trends. E_a values were increased with the increase of α , reaches a plateau about $\alpha = 0.2$, then the values of E_a were randomly scattered over the $0.2 < \alpha < 0.85$ values, and at $\alpha > 0.85$ the E_a values started descending with increasing the reaction front.

Figure 7: Variations of logarithmic values of the rates of thermal decomposition of PC-PET at a given α ($\ln R_\alpha$) versus it corresponding temperature ($1000/T_\alpha$) according to the Friedman method, Eq(15).

Kissinger-Akahira-Sunose

The Kissinger-Akahira-Sunose method (KAS) [48] employs the same equations as the Kissinger method Eq. (13) but replaces T_{max}

with T_α . The latter is the temperature related to a given conversion at different heating rates. Figure 8 shows the graphic representations of $\ln(\beta T_\alpha^{-2})$ versus $1000/T_\alpha$ based on the KAS method, Eq (15). The slope of the lines in the plot results in the value of $-E_{a,\alpha}/R$; the obtained values of $\langle E_a \rangle = 185 \pm 4$ kJ/mol were tabulated in the 4th column of table 4. The intercept of these lines which is a combination of $\ln A$ and $\ln f(\alpha)$ are tabulated in the 5th column of table 4; they are close to each other with standard deviations of ± 0.7 . If we assume that for a given reaction the value of $\ln A$ is constant for all α values; therefore, we must assume that the decomposition follows dissimilar $f(\alpha)$ values as the value of the function of the $f(\alpha)$ depend on the form and value of α , which is within expectations.

Figure 8: Variations of $\ln(\beta T_\alpha^{-2})$ versus it corresponding temperature ($1000/T_\alpha$) according to the KAV method, Eq. (14).

Figure 6 compares the E_a values obtained at each α with each other and with the one obtained from the modeled methods (section 5.4.1) and the Friedman method (section 5.4.2). As figure 6 shows, the values of E_a of PC-PET obtained from the KAS method were lower than the ones obtained from the previous methods but following a similar trend.

The Ozawa-Flynn-Wall

The Flynn-Wall-Ozawa (OFW) method is a model-free isoconversional method that has been used frequently to evaluate E_a of pyrolysis processes over α ranges based on equation 16. The slope of the straight line of a plot of $\ln \beta$ versus $1/T_\alpha$ gives $1.0518E_a/R$ (where R is the universal gas constant, and T_α corresponds to the temperature of decomposition at that particular α value) as shown in figure 9. The values of the $\ln A$,

and the E_a obtained from this method are tabulated in the 6th and 7th columns of table 4. The apparent $E_a = 187 \pm 4$ kJ/mol value obtained from the OFW method is close to the value of 166-180 kJ/mol obtained with the same method by Osma, *et al* [25]. Also, our E_a values obtained by OFW were about 1% higher than the values obtained from KAS method being $E_a = 185 \pm 4$ kJ/mol (section 4.4.3). The values of $\ln A = 29.39 \pm 0.67$ were much lower than the value of $\ln A = 30.36$ obtained from the KAS method. The large difference in the values of $\ln A$ is justified due to the assumptions that each method imbibed in the intercept.

which is slightly below our values of 187 ± 7 kJ/mol. The estimated E_a of PET by Martin-Gullon, *et al*. [50] were between 186-203 kJ/mol which is slightly above our values. Therefore, the E_a values obtained in this work are within the reported values and agreed by the values obtained by other researchers.

The activation energy obtained at various extents of reaction did not depend on the form of $f(\alpha)$ and the values of E_a obtained using any of the $f(\alpha)$ tabulated in table 1s agreed with each other within a statistical standard deviation of less than 1 kJ/mol, as indicated by the results tabulated in the last column of table 2s, as was the expectation. However, the value of the intercepts, $\ln A$, which describe the frequency of vibrations of the activated complex, depended on the α in the form of $f(\alpha)$, as shown in table 3s.

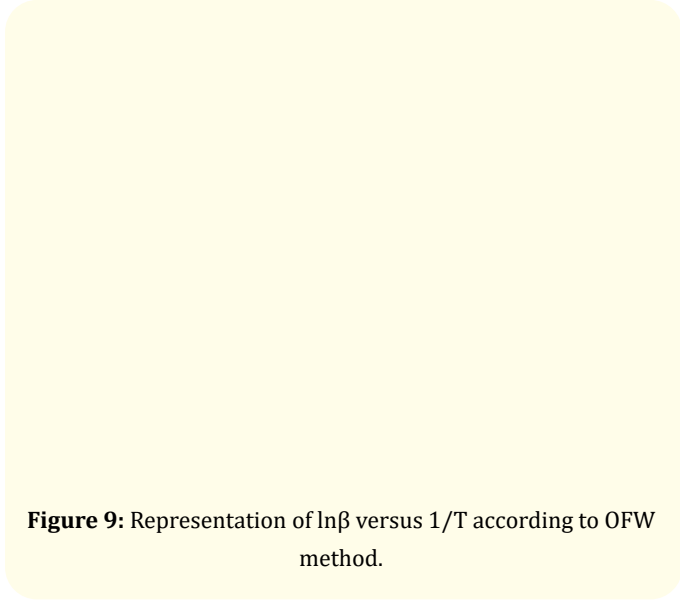


Figure 9: Representation of $\ln\beta$ versus $1/T$ according to OFW method.

Comparison, Conclusions and Remarks

The values of E_a of PC-PET increase by increasing the extent of reaction, it reached a plateau at $\alpha > 0.20$, but they had a descending trend at $\alpha > 0.85$, as shown in figure 6. The parameters of E_a and $\ln A$ obtained from the Friedman method were close to the model-free methods with a particular $f(\alpha)$. The lowest values of E_a belong to the KAS method (about 3% differences). The exception was $\alpha \geq 0.90$ where the values of E_a of F and $f(\alpha)$ models were lower than KVS, and FWO methods. The variation of E_a with the progression of the reaction front could be caused by the change in nature of the reactants by temperature. The clear PC-PET under heating decomposes to gaseous products and the porous dark surface layer of the degraded material which grows by α both in thickness and area. The heating process changes the nature of reactants and affects the transfer of heat into the reactants. The effects of heat transfer could be neglected, considering all samples had a similar weight and shape.

The overall activation energy of a commercial grade of PET studied by Al-Salem and Lettieri [49] was estimated to be 180.02 kJ/mol

No.	Reaction Model	Code	$f(\alpha)$
1	Power law	P4	$4\alpha^{3/4}$
2	Power law	P3	$3\alpha^{2/3}$
3	Power law	P2	$2\alpha^{1/2}$
4	Power law	P2/3	$2/3\alpha^{1/2}$
5	One-dimensional diffusion	D1	$1/2\alpha^{-1}$
6	Mampel (first order)	F1	$(1 - \alpha)$
7	Avrami-Erofeev	A4	$4(1 - \alpha)[- \ln(1 - \alpha)]^{3/4}$
8	Avrami-Erofeev	A3	$3(1 - \alpha)[- \ln(1 - \alpha)]^{2/3}$
9	Avrami-Erofeev	A2	$2(1 - \alpha)[- \ln(1 - \alpha)]^{1/2}$
10	Three-dimensional diffusion	D3	$3/2(1 - \alpha)^{2/3}[1 - (1 - \alpha)^{1/3}]^{-1}$
11	Contracting sphere	R3	$3(1 - \alpha)^{2/3}$
12	Contracting cylinder	R2	$2(1 - \alpha)^{1/2}$
13	Two-dimensional diffusion	D2	$[- \ln(1 - \alpha)]^{-1}$
14	Random Scission	L2	$2(\alpha^{1/2} - \alpha)$

Table 1S: Some of the kinetic models frequently used in the literature for solid-state kinetics; including a number related to the reaction model, the reaction model name, the code of the reaction model, and the integrated value of the function related to the reaction model, $f(\alpha)$.

The normalized rate of decomposition of the PC-PET, using \check{R}/R_{max} , as the reaction coordinate, is plotted as a function of temperature in Figure 2s for the five heating rates. A family of identical curves, similar to pure PET films, were displaced from one another on the temperature axis, similar to those in Figure 1b. From the similarity of the normalized reaction rates at the different heating rates, a single decomposition reaction mechanism for each heating rate could be suggested. (A priori, it could be the same or five different reaction mechanisms).

Model	1	2	3	4	5	6	7	8	9	10	11	12	13	14	Average	STDVE
α	P4	P3	P2	P2/3	D1	F1	A4	A3	A2	D3	R3	R2	D2	L2		
0.05	183.4	183.5	183.6	184.2	184.6	183.9	183.4	183.5	183.6	184.6	183.9	183.9	184.6	183.7	183.9	0.5
0.10	191.6	191.6	191.6	191.6	191.5	191.6	191.6	191.6	191.6	191.5	191.6	191.6	191.5	191.6	191.6	0.0
0.20	189.1	189.1	189.1	189.2	189.2	189.1	189.1	189.1	189.1	189.2	189.1	189.1	189.2	189.1	189.1	0.0
0.30	195.7	195.7	195.7	195.8	195.8	195.8	195.7	195.7	195.7	195.9	195.8	195.8	195.8	195.8	195.8	0.1
0.40	185.4	185.4	185.4	185.6	185.7	185.7	185.5	185.5	185.5	185.8	185.6	185.6	185.8	185.6	185.6	0.1
0.50	193.2	193.2	193.2	193.3	193.3	193.3	193.2	193.2	193.3	193.4	193.3	193.3	193.4	193.3	193.3	0.1
0.60	192.0	192.0	192.0	191.9	191.9	191.9	192.0	191.9	191.9	191.9	191.9	191.9	191.9	191.9	191.9	0.0
0.65	192.5	192.5	192.6	192.7	192.8	193.0	192.7	192.8	192.8	193.1	192.9	192.8	193.0	192.9	192.8	0.2
0.70	186.5	186.5	186.5	186.7	186.7	186.9	186.7	186.7	186.8	187.0	186.8	186.8	186.9	186.9	186.7	0.1
0.80	192.3	192.4	192.4	192.6	192.7	193.4	193.0	193.1	193.2	193.6	193.1	193.0	193.1	193.4	193.0	0.4
0.90	193.2	193.2	193.1	193.0	193.0	192.0	192.3	192.3	192.2	192.0	192.3	192.5	192.6	192.0	192.6	0.5
0.95	169.4	169.4	169.4	169.4	169.4	169.8	169.7	169.7	169.7	169.7	169.6	169.6	169.5	169.8	169.6	0.2
AVRG	189	189	189	189	189	189	189	189	189	189	189	189	189	189	188.8	0.1
STDV	7	7	7	7	7	7	7	7	7	7	7	7	7	7	7	

Table 2s: The E_a values for the corresponding α values evaluated from the related $f(\alpha)$ function of the models of table 2.

Model	1	2	3	4	5	6	7	8	9	10	11	12	13	14	Average	STDVE
α	P4	P3	P2	P2/3	D1	F1	A4	A3	A2	D3	R3	R2	D2	L2		
0.05	34.655	34.703	34.631	32.860	31.713	33.947	34.691	34.742	34.674	30.385	32.829	33.225	31.049	34.902	33.500	1.53
0.10	35.694	35.789	35.810	34.602	33.736	35.455	35.759	35.859	35.889	32.454	34.321	34.709	33.095	36.189	34.954	1.17
0.20	34.820	34.974	35.112	34.608	34.094	35.228	34.962	35.125	35.282	32.930	34.055	34.423	33.511	35.707	34.631	0.76
0.30	35.597	35.785	35.993	35.905	35.599	36.457	35.828	36.032	36.269	34.572	35.237	35.582	35.082	36.797	35.767	0.57
0.40	33.601	33.814	34.070	34.273	34.113	34.840	33.937	34.171	34.469	33.241	33.567	33.885	33.671	35.089	34.053	0.50
0.50	34.621	34.852	35.144	35.565	35.514	36.207	35.079	35.338	35.686	34.818	34.872	35.160	35.154	36.391	35.314	0.52
0.60	34.133	34.377	34.697	35.282	35.313	36.045	34.728	35.008	35.398	34.807	34.643	34.896	35.041	36.182	35.039	0.57
0.65	34.064	34.318	34.657	35.355	35.443	36.256	34.793	35.090	35.512	35.118	34.789	35.010	35.252	36.362	35.144	0.64
0.70	32.919	33.179	33.529	34.294	34.415	35.313	33.754	34.061	34.505	34.229	33.795	33.991	34.286	35.400	34.119	0.70
0.80	33.403	33.676	34.050	34.964	35.160	36.418	34.602	34.937	35.438	35.429	34.730	34.841	35.224	36.465	34.953	0.88
0.90	32.561	32.838	33.223	34.195	34.420	35.969	34.018	34.369	34.900	34.991	34.165	34.218	34.606	36.001	34.320	1.00
1	27.312	27.596	27.993	29.044	29.308	31.730	29.503	29.884	30.476	30.667	29.609	29.503	29.783	31.742	29.582	1.34
Ave	33.615	33.825	34.076	34.246	34.069	35.322	34.305	34.551	34.875	33.637	33.884	34.120	33.813	35.602	34.281	0.61
STDV	1.0	1.0	0.9	0.8	1.1	0.8	0.7	0.6	0.6	1.5	0.7	0.7	1.3	0.6		

Table 3s: The value of $\ln A$ for each α corresponding to the respective models indicated in table 2.

α	FM		KAS		FWO	
	Ea (kJ/mol)	lnA	Ea (kJ/mol)	ln A	Ea (kJ/mol)	ln(A)
0.05	183.9	36.88	175.5	30.45	177.4	25.48
0.10	191.6	37.65	180.8	30.89	182.6	25.89
0.20	189.1	36.61	186.2	31.30	187.9	26.27
0.30	195.8	37.30	186.9	31.04	188.6	26.02
0.40	201.8	37.94	187.2	30.82	189.0	25.82
0.50	193.2	36.19	187.4	30.64	189.3	25.65
0.60	192.0	35.64	187.9	30.51	189.9	25.53
0.65	192.7	35.58	187.5	30.35	189.5	25.37
0.70	186.6	34.41	187.8	30.29	189.8	25.32
0.80	189.0	34.28	186.2	29.78	188.4	24.85
0.90	181.8	32.04	185.9	29.43	188.2	24.51
0.95	176.0	29.82	184.2	28.82	186.7	23.94
Average	189	35.36	185	3.00	187	25.39
STAD	7	2.4	4	0.7	4	0.7

Table 4s: The values of E_a and lnA were obtained from KAS, FM, and FWO methods.

Acknowledgments

The authors declare no competing financial interest. In addition, they are grateful for the supports of Dr. Judith Sally, and Dr. Louis Whitesides. Any opinions, findings, and conclusions, or recommendations expressed in this material are those of the author and do not necessarily reflect those of the Funding Agencies.

Funding Support

This work was supported by the U.S. Department of Agriculture, National Institute of Food and Agriculture, Evans-Allen project number SCX-311-21-17 and SCX-311-29-21.

Bibliography

- Cooney JD., et al. "Thermal degradation of poly (ethylene terephthalate): a kinetic analysis of thermogravimetric data". *Journal of Applied Polymer Science* 28 (1983): 2887-2902.
- Geyer R., et al. "Production, use, and fate of all plastics ever made". *Science Advances* 3 (2017): 1-5 e1700782.
- Facts and Figures about Materials, Waste and Recycling. Plastics: Material-Specific Data (2020).
- Hamidi N., et al. "Pyrolysis of Household Plastic Wastes". *British Journal of Applied Science and Technology* 3 (2013): 417-439.
- Xu X., et al. "Degradation of poly (ethylene terephthalate)/clay nanocomposites during melt extrusion: Effect of clay catalysis and chain extension". *Polymer Degradation and Stability* 94 (2009): 113-123.
- Sovová K., et al. "A study of thermal decomposition and combustion products of disposable polyethylene terephthalate (PET) plastic using the high-resolution Fourier transform infrared spectroscopy, selected ion flow tube mass spectrometry and gas chromatography mass spectrometry". *Molecular Physics* 106 (2008): 1205-1214.
- Samperi F., et al. "Thermal degradation of poly (ethylene terephthalate) at the processing temperature". *Polymer Degradation and Stability* 83 (2004): 3-10.
- Romão W., et al. "Poly (ethylene terephthalate) thermo-mechanical and thermo-oxidative degradation mechanisms". *Polymer Degradation and Stability* 94 (2009): 1849-1859.
- Liu NA., et al. "Kinetic modeling of thermal decomposition of natural cellulosic materials in air atmosphere". *Journal of Analytical and Applied Pyrolysis* 63 (2002): 303-325.
- Jakab E., et al. "Thermogravimetry/mass spectrometry study of six lignins within the scope of an international round robin test". *Journal of Analytical and Applied Pyrolysis* 35 (1995): 167-179.
- Werner K., et al. "Thermal decomposition of hemicelluloses". *Journal of Analytical and Applied Pyrolysis* 110 (2014): 130-137.
- Cordero T., et al. "Thermal decomposition of wood in oxidizing atmosphere. A kinetic study from non-isothermal TG experiments". *Thermochimica Acta* 191 (1991): 161-178.
- Guindos P., et al. "Experimental and Numerical Characterization of the Influence of a Smoldering Cellulosic Substrate on a Cigarette's Ignition Propensity Test". *Fire Technology* 54 (2018): 669-688.
- Rogers FE and Ohlemiller TJ. "Cellulosic insulation material I. Overall degradation kinetics and reaction heats". *Combustion Science and Technology* 24 (1980): 129-137.

15. Thipkhumthod P, *et al.* "Pyrolytic characteristics of sewage sludge". *Chemosphere* 64 (2006): 955-962.
16. Jenekhe SA, *et al.* "Kinetics of the thermal degradation of poly (ethylene terephthalate)". *Thermochimica Acta* 61 (1983): 287-299.
17. Zimmerman H and Kim N T. "Investigations on thermal and hydrolytic degradation of poly (ethylene terephthalate)". *Polymer Engineering and Science* 20 (1980): 680-683.
18. Osman A I, *et al.* "Pyrolysis kinetic modelling of abundant plastic waste (PET) and in-situ emission monitoring". 32 (2020): 112.
19. Wu Y and Dollimore D. "Kinetic studies of thermal degradation of natural cellulosic materials". *Thermochimica Acta* 324 (1998): 49-57.
20. Chrissafis K. "Kinetics of thermal degradation of polymers complementary use of isoconversional and model-fitting methods". *Journal of Thermal Analysis and Calorimetry* 95 (2009): 273-283.
21. Criado JM, *et al.* "Correlation between the shape of controlled-rate thermal analysis curves and the kinetics of solid-state reactions". *Thermochimica Acta* 157 (1990): 171-179.
22. Ozawa T. "Temperature control modes in thermal analysis". *Journal of Thermal Analysis and Calorimetry* 64 (2001): 109-126.
23. Ozawa T. "Controlled rate thermogravimetry: New usefulness of controlled rate thermogravimetry revealed by decomposition of polyimide". *Journal of Thermal Analysis and Calorimetry* 59 (2000): 375-384.
24. Vyazovkin S, *et al.* "ICTAC Kinetics Committee recommendations for analysis of multi-step kinetics". *Thermochimica Acta* 689 (2020): 178597-178619.
25. Vyazovkin S, *et al.* "ICTAC Kinetics Committee recommendations for collecting experimental thermal analysis data for kinetic computations". *Thermochimica Acta* 590 (2014): 1-23.
26. Georgieva V, *et al.* "Non-Isothermal Degradation Kinetics of CaCO₃ from Different Origin". *Journal of Chemistry* 2013 (2012): 2090-9063.
27. Perejón A, *et al.* "Kinetic analysis of complex solid-state reactions. A new deconvolution procedure". *The Journal of Physical Chemistry B* 115 (2011): 1780-1791.
28. Redhead PA. "Thermal desorption of gases". *Vacuum* 12 (1962): 203-211.
29. Kissinger HE. "Variation of peak temperature with heating rate in differential thermal analysis". *Journal of Research of the National Bureau of Standards* 57 (1956): 217-221.
30. Doyle C. "Estimating Isothermal Life from Thermogravimetric Data". *Journal of Applied Polymer Science* 6 (1962): 639-642.
31. Sohoni GB and Mark JE. "Thermal stability of in situ filled siloxane elastomers". *Journal of Applied Polymer Science* 45 (1992): 1763-1775.
32. Abate L, *et al.* "Thermal stability of a novel poly (ether ether ketone ketone) (PK99)". *Polymer Engineering and Science* 36 (1996): 1782-1788.
33. Rao MPR, *et al.* "Thermal degradation kinetics of phenol-crotonaldehyde resins". *Polymer Degradation and Stability* 61 (1998): 283-288.
34. Brems A, *et al.* "Polymeric cracking of waste poly (ethylene terephthalate) to chemicals and energy". *Journal of the Air and Waste Management Association* 61 (2011): 721-731.
35. Hamidi N. "Kinetics study of the thermal decomposition of post-consumer poly (ethylene terephthalate) in an argon atmosphere". *Journal of Macromolecular Science, Part B* 58.2 (2019): 219-247.
36. Bockhorn H, *et al.* "Kinetic study on the thermal degradation of polypropylene and polyethylene". 48 (1999): 93-109.
37. Wang H, *et al.* "Thermal Degradation of Polystyrene under Extreme Nanoconfinement". *ACS Macro Letters* 8.11 (2019): 1413-1418.
38. Chattopadhyay J, *et al.* "Thermogravimetric characteristics and kinetic study of biomass co-pyrolysis with plastics". *Korean Journal of Chemical Engineering* 25 (2008): 1047-1053.
39. Dollimore D, *et al.* "The use of the rising temperature technique to establish kinetic parameters for solid-state decompositions using a vacuum microbalance". *Thermochimica Acta* 24 (1978): 293-306.

40. Gallagher PK., *et al.* "Kinetics of the thermal decomposition of CaCO₃ in CO₂ and some observations on the kinetic compensation effect". *Thermochimica Acta* 14 (1976): 255-261.
41. Saha B and Ghoshal A K. "Thermal degradation kinetics of poly (ethylene terephthalate) from waste soft drinks bottles". *Chemical Engineering Journal* 111 (2005): , 39-43.
42. Smith J M. "Chemical Engineering Kinetics". McGraw-Hill, 3rd ed. (1981): 392.
43. Vyazovkin S. "Kissinger Method in Kinetics of Materials: Things to Beware and Be Aware of Molecules". 25 (2020): , 2813-2831.
44. Du S., *et al.* "Conversion of Polyethylene Terephthalate Based Waste Carpet to Benzene-Rich Oils through Thermal, Catalytic, and Catalytic Steam Pyrolysis". *ACS Sustainable Chemistry and Engineering* 4 (2016): 2852-2860-2860.
45. Vyazovkin S. "Kinetic concepts of thermally stimulated reactions in solids: A view from a historical perspective". *International Reviews in Physical Chemistry* 19 (2000): 45-60.
46. Vyazovkin S. "On the phenomenon of variable activation energy for condensed phase reactions". *New Journal of Chemistry* 24 (2000): 913-917.
47. Atkins P and de Paula J. "Physical Chemistry" (9th ed.) W.H. Freeman, New York (Discussion of negative activation energies is also found in other editions, see subject index under "activation energy, negative") (2010).
48. Akahira T and Sunose T. "Method of determining activation deterioration constant of electrical insulating materials". 16 (1971): 22-31.
49. SM Al-Salem and P Lettieri. *World Academy of Science, Engineering and Technology* 42 (2010): 1253-1261
50. Martin-Gullon I., *et al.* "Kinetic model for the pyrolysis and combustion of poly (ethylene terephthalate) (PET)". *Journal of Analytical and Applied Pyrolysis* (2001): 58-59; 635-650.

Volume 1 Issue 1 September 2021

© All rights are reserved by Nasrollah Hamidi and Nurannahaar Abdussalam.